2023 IEEE Symposium Series on Computational Intelligence (SSCI)
Mexico City, Mexico. December 5-8, 2023

Enhancing Content-Based Histopathology Image Retrieval Using QR Code Representation

Hamidreza Rouzegar
Department of Electrical, Computer, and Software Engineering
Ontario Tech University
Oshawa, ON, Canada
hamidreza.rouzegar@ontariotechu.net

Shahryar Rahnamayan,SMIEEE
Engineering Department
Brock University
St. Catharines, ON, Canada
srahnamayan@brocku.ca

Azam Asilian Bidgoli
Faculty of Science
Wilfrid Laurier University
Waterloo, ON, Canada
abidgoli@wlu.ca

Masoud Makrehchi
Department of Electrical, Computer, and Software Engineering
Ontario Tech University
Oshawa, ON, Canada
masoud.makrehchi@ontariotechu.net

***Abstract*— The growing field of Content-Based Medical Image Retrieval (CBMIR) plays an integral role in the diagnosis and treatment plan of numerous diseases, including cancer. However, the effective representation of gigapixel medical images via a large number of extracted features remains a challenging task, crucially influencing other processes in a digital workflow. In this paper, we propose a novel QR code representation strategy to enhance retrieval performance. Unlike the traditional one-dimensional binary representation methods (i.e., barcodes), this 2D approach captures more intricate and informative patterns from the features by differentiating each pair of features resulting in a 2D binary vector. We delve into three distinct QR code generation strategies, namely, the Thresholding QR, the MinMax QR, and the Hybrid QR, each offering unique strengths. Our experiments on representing whole slide images of the Cancer Genome Atlas (TCGA) dataset reveal that while the Hybrid QR tends to provide balanced performance, there are instances where the other two methods outshine. Even though this approach requires more memory usage, the considerable enhancement in accuracy justifies this trade-off; obviously, in medical applications, accuracy holds the highest priority. Hence, the findings indicate that QR codes can effectively improve the performance of CBMIR systems by not only accelerating the retrieval process but also increasing the accuracy of image retrieval, leading to potentially more accurate diagnoses and treatment planning.**

Keywords*— *Content-Based Image Retrieval, Histopathology Images, Barcode, QR Code, Medical Image Analysis

I. INTRODUCTION

The central objective of medical information systems, consistently defined across a plethora of research, has been providing timely, location-appropriate, and person-specific information. The aim is to elevate the standards of healthcare delivery, augmenting the quality of care processes and simultaneously bolstering their efficiency [1]. In recent years, medical imaging and processing have been identified as an invaluable aid in healthcare. Emerging as a critical component in diagnostic processes, medical imaging, and processing are contributing significantly to the efficient and accurate delivery of healthcare services [2].

Imaging technology has evolved dramatically over the years, making it an indispensable asset in a wide range of medical scenarios. It plays a pivotal role in the diagnosis, treatment, and monitoring of various health conditions [3]. This has prompted the development and integration of computer-aided diagnostics into radiological practice, a trend underscored by exhibits and demonstrations at the Radiological Society of North America (RSNA) [4].

Despite the significant strides made in imaging technology, a pressing challenge is the identification of essential tasks in medical imaging based on their potential clinical benefits. Purely visual image queries, as executed in the computer vision domain, are unlikely to entirely supplant text-based methods. However, visual queries hold immense potential to serve as a complementary tool to text-based searches [5]. To fully exploit the advantages of both visual and text-based access methods, it is vital to address their inherent challenges and underscore their unique benefits.

One of the key technologies that have emerged to address these challenges is Content-Based Image Retrieval (CBIR). CBIR represents an advanced method for image search, specifically designed to identify images in large databases that closely match a given query image [6]. CBIR assesses the similarity between images based on the properties of their visual components, including color, texture, shape, and spatial arrangement of regions of interest (ROIs). This approach eliminates the dependence on labels, proving particularly useful for expansive repositories where manual assignment of keywords and annotations may prove impractical [7]. Various strategies have been adopted to determine the similarity of image features, such as Euclidean distance metrics, concepts of elastic deformation, graph matching, and statistical classifiers [8]. A fast and accurate image retrieval is very helpful and appreciated in many research and operational fields.

In order to process an image in a digital workflow, discriminative features should be extracted to represent the image. Image representation has witnessed remarkable progress over the past two decades, spanning two significant periods, namely feature engineering and deep learning. During the era of feature engineering, various innovative handcrafted image representations like SIFT [9] and Bag of Visual Words (BoW) [10] dominated the field. More recently, the age of deep learning has ushered in a new wave of

approaches, such as fine evolutionary feature selection combined with pre-trained Deep Neural Networks (DNNs) for more efficient feature extraction, especially from large-scale images such as Whole Slide Images (WSIs) in digital pathology [11], [12].

Due to the large number of features representing a typical image, expensive computation and a massive amount of memory for image retrieval are required. Binarization, a transformative process of converting numerical or categorical data into a binary form, stands out as a pivotal concept in this context. By symbolizing image features in a binary format, it becomes feasible to substantially diminish the computational and memory overhead. [13] To address the challenges of fast retrieval and low memory complexity in image representation scope, researchers have turned to unique solutions, such as the use of barcodes as a substitute for conventional image features. Such methods, which are essentially 1D binary representations, have included the use of Radon barcodes [14], Minmax radon barcodes [15], SVM-based approaches [16], and auto-encoded Radon barcodes [17]. Each of these methods has presented its own set of advantages and challenges. Obviously, the bitwise operations would be much faster and memory efficient, especially when we consider embedded systems.

Recently, the use of Quick Response QR codes, inherently binary and 2D in their representation, has been explored in the context of book retrieval [18] and to prevent Trojan-horse attacks [19]. QR codes present an opportunity to incorporate a larger quantity of feature information in a binary format akin to conventional barcodes (i.e., Data Capacity). The ability to preserve more feature information, albeit with a slight increase in memory usage, suggests that QR codes could potentially enhance retrieval accuracy in medical imaging applications.

This paper presents a pioneering exploration of the application of QR codes in the context of Content-Based Medical Image Retrieval (CBMIR), positioning QR codes as a potential substitute for conventional barcodes. The presented QR code is generated by differentiating each pair of features resulting in a 2D binary feature vector. We delve into a comprehensive comparison of the accuracy of two existing barcode models and three novel QR code models. This work, to the best of our knowledge, is the first scholarly attempt to integrate QR codes into CBMIR, and our findings underscore the significant improvement in retrieval accuracy enabled by our proposed method. The proposed scheme has very little computational burden, which is negligible.

The remainder of this paper is structured as follows: Section II introduces our proposed method of integrating QR codes into CBMIR. Section III outlines the computational experiments and subsequent analysis used to test our method. Section IV presents and discusses our findings, comparing our approach against traditional barcode models. Finally, Section V provides a summary of our results and their implications, concluding with suggestions for future research.

II. Existing Barcode Methods

Within the domain of Content-Based Image Retrieval (CBIR), the endeavor of translating intricate features into accessible binary codes has been a point of academic exploration. Conventionally, the method of choice for this purpose has been the barcode. While efficient in terms of memory usage and simplicity of interpretation, barcodes operate within the limitations of a one-dimensional paradigm.

This research seeks to push past the constraints of this 1D space. The core hypothesis of our study suggests that elevating the binary representation into a two-dimensional space could potentially result in more accurate and refined data retrieval. To address this, we have devised a novel system that evolves the 1D binary barcode into a 2D binary QR code. This expansion comes with the inherent trade-off of augmented memory consumption, a factor we have thoroughly examined. In the following, the data preparation phase and the various schemes of the proposed barcode or QR code generations are explained.

A. Barcode Generation Through Thresholding

Historically, one of the prevalent techniques for transforming feature vectors into binary barcodes has been thresholding [14]. This technique involves a process of standardization, wherein all features are normalized to a range between 0 and 1. As the post-normalization, the binary assignment occurs through a comparison with the mean value (0.5); feature values lower than the mean are translated into a binary '0', and values higher than the mean are translated into a binary '1'. This process ensures a balanced distribution of binary values within the barcode. Of course, other thresholding methods can be utilized.

B. Generation of MinMax Barcodes

The simplicity and efficiency of the thresholding technique notwithstanding, it suffers from a significant shortcoming: it does not capture the dynamic transitions of feature values, overlooking the overall curvature of the feature projections. To address this gap, an evolved approach [15], referred to as the MinMax barcode, was proposed. This approach considers the relative changes between consecutive features. If a feature value in the vector exceeds its preceding feature, it is denoted by a binary '1'; if it is equal or lesser, it receives a binary '0'. This method ensures a more nuanced binary representation, capturing more information and thus providing a richer insight into the feature dynamics.

III. The Proposed Approach: QR Code Generation

With the stage set by these conventional barcode generation techniques, we introduced our pioneering QR code representation. This advanced approach, designed to significantly enhance the accuracy of the CBMIR system, extends upon the principles of both thresholding and MinMax techniques while introducing additional innovative processes. By introducing the QR code, in fact, we consider all pair-wise feature relationships, which would be independent of the ordering of the features in the barcode scheme. This approach will offer a richer representation which was not achievable by a barcode scheme. In the following, the details of three different variations of the proposed QR code are presented.

A. The Intricacies of Data Preparation and Feature Extraction

The beginning of our research hinges on image patch extraction from WSIs of publicly available TCGA[12]. Due to the extremely large dimensions of each WSI, a number of patches (135 on average) are required to be extracted from different regions of an image. In alignment with robust methodologies established in preceding research [12], we use patches that are distinctly unique and representative of our dataset. Each patch, encompassing 1000*1000 pixels at a 20x magnification, was selected to avoid any overlap with others.

Upon extraction, these patches have already been processed using KimiaNet, a deep neural network based on the DenseNet architecture, as detailed in [12]. KimiaNet architecture is four distinct dense blocks, each containing bespoke convolutional and pooling layers designed to maximize data processing efficacy. Through the workings of KimiaNet, each patch is represented by a 1024-dimensional feature vector, creating a high-dimensional space that encapsulates intricate patterns within the images.

It's important to note that our research doesn't involve the feature extraction and preprocessing stages. Instead, we use the extracted features from the WSIs of the TCGA dataset in [12] and make an innovative departure from conventional techniques by employing a center-based sampling approach during our analyses. We utilized the mean of all feature vectors within a single WSI to drastically simplify the complex multidimensional space. This process allows us to condense the information from the separate vectors per WSI into a single, coherent, 1024-dimensional vector, enabling a more streamlined subsequent analysis and computation.

B. Thresholding QR Code

The first variant of our QR code technique adapts the threshold-based barcode approach but includes a key variation: it evaluates the absolute difference between each pair of features, creating a matrix of these differences. Following the calculation of differences, these values are normalized between 0 and 1. Cells within the matrix that hold a value higher than the mean difference are assigned a binary '1', while cells with a value lower than the mean difference receive a binary '0'. This approach preserves the relationships between all features and potentially offers a richer, more discriminative information set for the CBMIR system. We begin by creating a difference matrix 'D', where each entry D(i, j) represents the absolute difference between features f(i) and f(j) for all i, j such that $1 \leqslant j < i \leqslant n$. This triangular matrix is a result of acknowledging that D(i, j) = D(j, i); hence only half the matrix needs to be computed.

$$D(i,j) = |f(i) - f(j)| \tag{1}$$

The next step is to normalize the difference matrix 'D' by dividing each entry by the maximum value in 'D', generating a normalized matrix 'N'.

$$N = D/Max(D) \tag{2}$$

In the final step, a thresholding operation is applied to 'N' to generate our QR code matrix 'Q'. Any cell within 'N' that holds a value greater than the mean value of 'N' is assigned a binary '1' in 'Q'. Conversely, any cell with a value less than or equal to the mean value receives a binary '0' in 'Q'.

$$Q(i,j) = \begin{cases} 1 & \text{if } N(i,j) > mean(N) \\ 0 & \text{if } N(i,j) \leq mean(N) \end{cases} \tag{3}$$

Through this process, our approach preserves the relationships between all features and potentially offers a richer, more discriminative information set for the Content-Based Medical Image Retrieval (CBMIR) system. It should be noted that the remaining half of 'Q' (i.e., where $j \geqslant i$) can be filled with 0's or simply left undefined as those values are not used, further enhancing computational efficiency.

C. MinMax QR Code

Our second QR code variant mirrors the concepts underpinning the MinMax barcode. In this method, a 1024*1024 binary matrix is formed. Each cell within this matrix represents a comparison between its corresponding row and column values. If the row value surpasses the column value, the cell is annotated with a binary '1'. If it's equal or lesser, the cell is marked with a binary '0'. This method successfully conserves the comparative dynamics between every pair of features, possibly providing a more sophisticated level of detail for the CBMIR system.

Just as with the first QR code variant, we are only interested in the upper triangular part of the matrix as Q(i, j) = not Q(j, i). As such, we can also limit our computations to half the matrix. The steps involved in the formation of the MinMax QR Code are as follows:

Start by creating a 1024*1024 binary matrix 'C'. In this matrix, each cell Q(i, j) is a comparison between features f(i) and f(j) for all i, j such that $1 \leqslant i < j \leqslant n$. If the row value f(i) is strictly greater than the column value f(j), the cell is annotated with a binary '1'. Conversely, if f(i) is equal to or less than f(j), the cell is marked with a binary '0'.

$$Q(i,j) = \begin{cases} 1 & \text{if } f(i) > f(j) \\ 0 & \text{if } f(i) \leq f(j) \end{cases} \tag{4}$$

Through this method, the MinMax QR Code successfully establishes a binary map that characterizes the comparison of each unique pair of features. Importantly, only less than half of the cells in the matrix are used in the computation, with the rest being redundant due to the symmetry of comparison. If x > y, then we can confidently state that y <= x, and there is no need to compute or store this information again. This strategy provides a significant improvement in the computational efficiency of the method.

D. Hybrid QR Code

In this version, we take advantage of the symmetry of our square feature matrix and apply two different algorithms on the upper and lower halves of the matrix. We divide the matrix along its main diagonal, with the cells above the main diagonal (excluding the diagonal itself) adhering to the Comparison Matrix methodology, while those below the diagonal employ the Thresholding QR method.

The cells on the main diagonal, forming the boundary between the two distinct halves, are uniformly assigned a binary '0', forming a clear partition between the two methodologies.

It should be noted that while the Hybrid QR Code capitalizes on the strengths of both the Comparison and Thresholding QR code methods, it also demands twice the memory capacity due to the storage of two sets of information. This increase in memory usage is an important factor to consider when evaluating the feasibility of this QR code variant. Incorporating these three QR code techniques into our novel methodology has allowed us to probe deeper into the potential trade-offs between increased memory usage and improved retrieval accuracy within the context of CBMIR systems. Our comprehensive results provide valuable insights into the efficacy of these innovative methods and set the foundation for further exploration and application in the CBMIR domain. The process is demonstrated in Fig. 1.

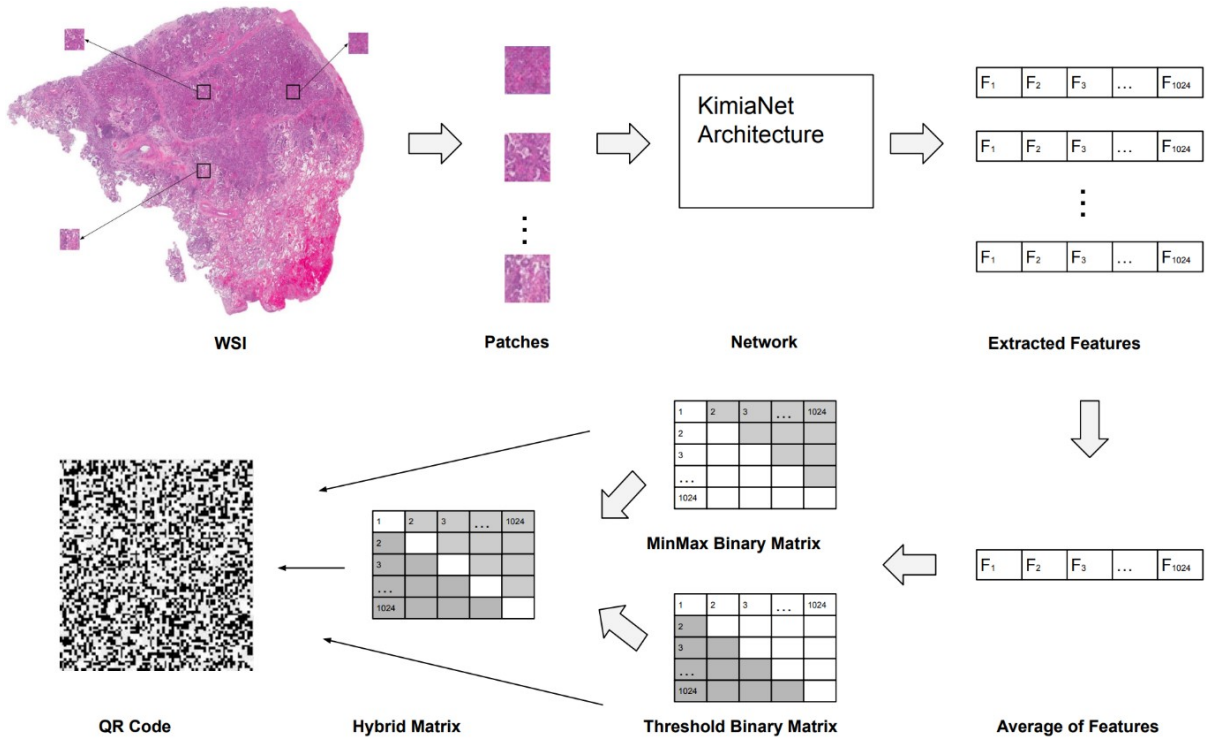

Fig. 1. Diagrammatic representation of the proposed framework - This figure illustrates the workflow from WSI extraction, where individual patches are extracted, and processed through the KimiaNet to extract the feature vectors. The mean of these vectors is used to form matrices using MinMax binary, Threshold binary methods, and a combination of the two That is Hybrid Matrix. These matrices are further transformed into their respective QR code representations.

IV. Experiments and Analysis

The following sections will provide an in-depth exploration of our experimentaly conducted tests and findings. We will take a closer look at the performance metrics of each method we've employed, drawing comparisons and making interpretations based on the data at hand. As evidenced by the detailed assessments presented in the subsequent sections, the efficacy of the approach we are proposing will be made apparent.

A. Image Retrieval Framework and Settings

In order to evaluate the performance of CBIR using the proposed QR code, we use the *k*-Nearest Neighbors (*k*-NN) classifier to find the most similar WSIs to a query image. This simple classifier, well-respected and widely used within the machine learning arena, operates by comparing an input sample with its closest neighbors within the feature space. It then assigns the class label based on the labels of these neighbors. However, the performance of this classifier greatly depends on the suitable selection of '*k*', the number of neighbors being considered.

Please note that in our case, we're employing the *k*-NN classifier to retrieve WSIs rather than individual patches to provide a more comprehensive view of the tumor. We tested the classifier with different '*k*' values to identify the optimal balance between precision and computational complexity, with detailed results discussed in the subsequent sections.

The objective of our study was to use the feature space effectively, acknowledging that different types of tumors could manifest distinctly in the high-dimensional space. We, therefore, structured our optimization problems around maximizing the performance of our classifier for each specific tumor type, given the feature representation provided by KimiaNet and our QR code methodology.

Our research methodology employs the leave-one-out approach, a widely accepted technique in data analysis, to achieve comprehensive and unbiased results. In this method, we select one image at a time from our dataset to serve as the test data, while the remaining images make up the retrieval training set. Then, '*k*' most similar images to the selected query image will be found among the training set.

This iterative process continues until each image in our dataset has served once as the query image. This approach ensures a rigorous assessment of our QR code methodologies, testing their effectiveness on every image in our dataset. It provides us with robust evaluation results, which are critical in validating the efficiency and reliability of our proposed techniques.

In our experiments, the *k* parameter is specifically set to 3. This choice was based on the understanding that a trio of neighbors provides a balanced perspective, minimizing the chance of a tie during class label prediction while also reducing the risk of overfitting that could be associated with a larger value of *k*.

When it comes to choosing a distance metric, we opted for the Hamming distance, which is particularly suitable for binary data. Hamming distance measures the number of bit positions where two binary strings differ. By using the Hamming distance, we intended to establish a robust comparative framework between the binary representations of image features. This method facilitated more accurate image retrieval from the dataset and contributed significantly to the efficacy of our approach. In order to compute the accuracy of

image retrieval using the real values of features and compare them with our method, we use Euclidian distance.

B. TCGA Dataset

The dataset for this research was primarily sourced from the TCGA dataset, a comprehensive repository renowned for its detailed genomic sequences of various cancer types. This ensures the credibility and accuracy of the samples used in our study. The selected dataset spans multiple cancer sites, with each site encompassing various tumor types and subtypes, making the dataset representative and diverse. These categories span a total of 8 primary tumor types, represented across 26 specific subtypes. This comprehensive variety ensures a well-rounded representation of diverse tumor variations. The in-depth breakdown of this dataset is illustrated in TABLE I.

TABLE I. DATASET DESCRIPTION - NUMBER OF SAMPLES ACROSS VARIOUS CANCER TYPES

Site	Cancer Type	#Samples
Brain	Brain Lower Grade Glioma	35
	Glioblastoma Multiforme	39
Endocrine	Adrenocortical Carcinoma	6
	Pheochromocytoma and Paraganglioma	15
	Thyroid Carcinoma	51
Gastrointestinal	Colon Adenocarcinoma	33
	Rectum Adenocarcinoma	11
	Esophageal Carcinoma	14
	Stomach Adenocarcinoma	30
Gynecological	Cervical Squamous Cell Carcinoma and Endocervical Adenocarcinoma	17
	Ovarian Serous Cystadenocarcinoma	10
	Uterine Carcinosarcoma	3
Liver	Cholangiocarcinoma	4
	Liver Hepatocellular Carcinoma	35
	Pancreatic Adenocarcinoma	12
Mesenchymal	Uveal Melanoma	4
	Skin Cutaneous Melanoma	24
Prostrate	Prostate Adenocarcinoma	40
	Testicular Germ Cell Tumors	13
Pulmonary	Lung Adenocarcinoma	43
	Lung Squamous Cell Carcinoma	38
	Mesothelioma	5
Urinary tract	Bladder Urothelial Carcinoma	34
	Kidney Chromophobe	11
	Kidney Renal Clear Cell Carcinoma	50
	Kidney Renal Papillary Cell Carcinoma	28

C. Result Analysis

The findings of our comprehensive experimental trials are outlined in TABLE II. reinforcing the effectiveness of our innovative QR code representation method for tumor classification. The first column of the table shows the retrieval accuracy using the original real-valued features. The three next columns represent the results of 1D barcode while the last three columns indicate the accuracy values of image retrieval using the three proposed QR codes. An observation from the reported results shows that the QR techniques, despite demanding an increased memory allocation compared to traditional methods, have demonstrated superior classification accuracy.

If we rank the methods based on mean accuracy, the MinMax QR shows the highest mean accuracy at 91.57%, indicating it as the most effective method across the majority of tumor types. For instance, in pulmonary category, the QR code is able to discriminate the cancer subtypes with 90.70% accuracy, which is the highest value among all competitors' results. Following closely, the Hybrid QR method yields a mean accuracy of 90.46%, showcasing a robust performance, while the Thresholding QR approach also displays commendable performance with a mean accuracy of 90.19%. The MinMax barcode and real-valued feature come next, delivering mean accuracies of 89.85% and 89.52%, respectively. The Thresholding barcode method shows the lowest mean accuracy at 87.53%.

The MinMax Barcode and mean feature methods come next, delivering mean accuracies of 89.85% and 89.52%, respectively. The Thresholding Barcode method shows the lowest mean accuracy at 87.53%.

Examining the standard deviation values gives insight into the consistency of each method across different tumor types. With the lowest standard deviation at 6.79, the MinMax QR method demonstrates the most consistent performance across all tumor categories. In contrast, the MinMax barcode method, having the highest standard deviation of 7.98, exhibits the most variation in its performance across different tumor types.

Each QR code generation strategy - the Thresholding QR, MinMax QR, and Hybrid QR - performs variably across the tumor categories. Although the Hybrid method generally displays a robust performance, there were cases where the Thresholding and MinMax QR methods outperformed it. Overall, all QR variants reach a higher accuracy than original real-valued features while they consume less memory resources leading to faster retrieval.

Conclusively, the QR code representation method shows promising potential in enhancing the classification accuracy of various tumor types. However, this does not discount the possibility of future advancements in the QR code generation strategies that could steer the field of tumor classification and, ultimately, cancer diagnosis and treatment in more promising directions.

V. CONCLUSION REMARKS

In this paper, we introduced a novel QR code-based representation for histopathology images. This approach is built on the concept of utilizing a 2D binary framework. It effectively captures the complex relationships among image features. This innovative representation preserves the inherent intricacies of the images. Our approach was centered on the premise that the relationships between every pair of features when captured, offer a richer dimensionality that can contribute to better differentiation and identification. Drawing a conclusion from the extensive experimental trials and thorough assessments carried out on the TCGA dataset, which encompasses a diverse range of tumor types and subtypes, the results substantiate the effectiveness of our novel approach - the QR code representation method. Despite the increase in memory utilization, the trade-off is justified by the substantial improvement in accuracy over the traditional 1D barcodes. It affirms that, by using a 2D binary representation system for image retrieval, we can capture more complex, and hence more informative, feature relationships than its one-dimensional counterpart (because all pair-wise feature relationships are captured). Moreover, this method provides

an edge over real-valued representations by offering faster retrieval times due to the nature of binary operations.

Through different QR code generation strategies - the MinMax QR, Thresholding QR, and Hybrid QR we observed varying degrees of performance. Each strategy has its strengths and distinctive attributes, and none is a universally superior solution across all tumor types. In the broader perspective of cancer research, this work has showcased the potential of QR codes as a tool for improving the accuracy of CBMIR systems, making them a valuable asset in the diagnostic process. Future work can explore further optimization of the QR code generation methods, developing more refined and sophisticated techniques to further improve system performance. The proposed scheme can be utilized for other medical or non-medical image modalities.

In conclusion, the use of QR codes as an alternative to traditional barcodes for feature representation in CBMIR promises better retrieval accuracy and opens up a new avenue for continued research in this field. Despite the challenges and trade-offs, the path forward seems promising and will likely contribute significantly to advancing medical image analysis.

TABLE II. MEAN ACCURACY AND STANDARD DEVIATION OF DIFFERENT FEATURE REPRESENTATION METHODS ACROSS VARIOUS TUMOR TYPES

Site	Mean Features	MinMax Barcode	Thresholding Barcode	MinMax QR	Thresholding QR	Hybrid QR
Brain	86.49	85.14	83.78	89.19	86.49	**90.54**
Endocrine	93.06	94.44	91.67	**95.83**	94.44	95.83
Gastrointestinal	76.14	72.73	73.86	76.14	**78.41**	76.14
Gynecological	96.88	96.88	87.50	96.88	**100.00**	96.88
Liver	86.27	86.27	**90.20**	86.27	88.24	86.27
Mesenchymal	92.86	96.43	92.86	**96.43**	92.86	92.86
Prostrate	**100.00**	**100.00**	98.11	**100.00**	**100.00**	**100.00**
Pulmonary	83.72	84.88	77.91	**90.70**	80.23	83.72
Urinary tract	90.24	91.87	91.87	**92.68**	91.06	91.87
Mean	89.52	89.85	87.53	**91.57**	90.19	90.46
Std	6.83	7.98	7.28	**6.79**	7.25	6.96

REFERENCES

[1] Winter, A., and R. Haux. "A Three-Level Graph-Based Model for the Management of Hospital Information Systems." Methods of Information in Medicine, vol. 34, no. 04, Georg Thieme Verlag KG, July 1995, pp. 378–96.

[2] Kahn, C. E. "Artificial Intelligence in Radiology: Decision Support Systems." RadioGraphics, vol. 14, no. 4, Radiological Society of North America (RSNA), July 1994, pp. 849–61.

[3] Doi, Kunio. "Computer-aided Diagnosis in Medical Imaging: Historical Review, Current Status and Future Potential." Computerized Medical Imaging and Graphics, vol. 31, no. 4–5, Elsevier BV, June 2007, pp. 198–211.

[4] Abe, Hiroyuki, et al. "Computer-aided Diagnosis in Chest Radiography: Results of Large-Scale Observer Tests at the 1996–2001 RSNA Scientific Assemblies." RadioGraphics, vol. 23, no. 1, Radiological Society of North America (RSNA), Jan. 2003, pp. 255–65.

[5] Sakila, A., and S. Vijayarani. "Content-Based Text Information Search and Retrieval in Document Images for Digital Library." Journal of Digital Information Management, vol. 16, no. 3, Digital Information Research Foundation, Jan. 2018, p. 136.

[6] Smeulders, A. W. M., et al. "Content-based Image Retrieval at the End of the Early Years." IEEE Transactions on Pattern Analysis and Machine Intelligence, vol. 22, no. 12, Institute of Electrical and Electronics Engineers (IEEE), 2000, pp. 1349–80.

[7] Kumar, Ashnil, et al. "Content-Based Medical Image Retrieval: A Survey of Applications to Multidimensional and Multimodality Data." Journal of Digital Imaging, vol. 26, no. 6, Springer Science and Business Media LLC, July 2013, pp. 1025–39.

[8] Akgül, Ceyhun Burak, et al. "Content-Based Image Retrieval in Radiology: Current Status and Future Directions." Journal of Digital Imaging, vol. 24, no. 2, Springer Science and Business Media LLC, Apr. 2010, pp. 208–22.

[9] Lowe, David G. "Distinctive Image Features From Scale-Invariant Keypoints." International Journal of Computer Vision, vol. 60, no. 2, Springer Science and Business Media LLC, Nov. 2004, pp. 91–110.

[10] Hong, Chaoqun, et al. "An Efficient Approach to Content-based Object Retrieval in Videos." Neurocomputing, vol. 74, no. 17, Elsevier BV, Oct. 2011, pp. 3565–75.

[11] Kalra, Shivam, et al. "Pan-cancer Diagnostic Consensus Through Searching Archival Histopathology Images Using Artificial Intelligence." Npj Digital Medicine, vol. 3, no. 1, Springer Science and Business Media LLC, Mar. 2020.

[12] Bidgoli, Azam Asilian, et al. "Evolutionary Computation in Action: Hyperdimensional Deep Embedding Spaces of Gigapixel Pathology Images." IEEE Transactions on Evolutionary Computation, vol. 27, no. 1, Institute of Electrical and Electronics Engineers (IEEE), Feb. 2023, pp. 52–66.

[13] Chaki, N., Shaikh, S.H., Saeed, K. "A Comprehensive Survey on Image Binarization Techniques." Exploring Image Binarization Techniques. Studies in Computational Intelligence, Springer India, May. 2014, pp. 5-15.

[14] H. R. Tizhoosh, "Barcode annotations for medical image retrieval: A preliminary investigation," 2015 IEEE International Conference on Image Processing (ICIP), Quebec City, QC, Canada, 2015, pp. 818-822.

[15] H. R. Tizhoosh, S. Zhu, H. Lo, V. Chaudhari, and T. Mehdi, "Minmax radon barcodes for medical image retrieval," in Advances in Visual Computing: 12th International Symposium, ISVC 2016, Las Vegas, NV, USA, December 12-14, 2016, Proceedings, Part I 12, pp. 617–627.

[16] S. Zhu and H. R. Tizhoosh, "Radon features and barcodes for medical image retrieval via SVM," in 2016 International Joint Conference on Neural Networks (IJCNN), pp. 5065–5071.

[17] H. R. Tizhoosh, C. Mitcheltree, S. Zhu, and S. Dutta, "Barcodes for medical image retrieval using autoencoded radon transform," in 2016 23rd International Conference on Pattern Recognition (ICPR), pp. 3150– 3155.

[18] F. Hu, A. Chen and X. Li, "Towards Making a Trojan-Horse Attack on Text-to-Image Retrieval," ICASSP 2023 - 2023 IEEE International Conference on Acoustics, Speech and Signal Processing (ICASSP), Rhodes Island, Greece, 2023, pp. 1-5.

[19] Wang, Qiuyan, and Dong Haibing. "Book Retrieval Method Based on QR Code and CBIR Technology." Journal on Artificial Intelligence, vol. 1, no. 2, Computers, Materials and Continua (Tech Science Press), 2019, pp. 101–110.